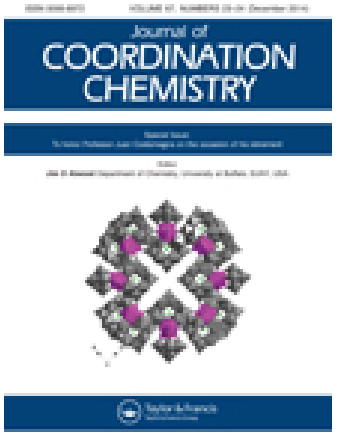

Journal of Coordination Chemistry
Publication details, including instructions for authors and subscription information:
http://www.tandfonline.com/loi/gcoo20

Coordination interactions in the crystalline lattice of alkaline ions with the polyoxometalate $[V_{12}B_{18}O_{60}H_6]^{10-}$ ligand

Patricio Hermosilla-Ibáñez[ab], Juan Costamagna[a], Andrés Vega[bc], Verónica Paredes-García[bc], Eric Le Fur[de], Evgenia Spodine[bf] & Diego Venegas-Yazigi[ab]

[a] Facultad de Química y Biología, Universidad de Santiago de Chile, Santiago, Chile

[b] CEDENNA, Santiago, Chile

[c] Facultad de Ciencias Exactas, Departamento de Ciencias Químicas, Universidad Andres Bello, Santiago, Chile

[d] ENSCR, CNRS, UMR 6226, Rennes, France

[e] Université Européenne de Bretagne, France

[f] Facultad de Ciencias Químicas y Farmacéuticas, Universidad de Chile, Santiago, Chile

Accepted author version posted online: 01 Sep 2014.Published online: 08 Oct 2014.

To cite this article: Patricio Hermosilla-Ibáñez, Juan Costamagna, Andrés Vega, Verónica Paredes-García, Eric Le Fur, Evgenia Spodine & Diego Venegas-Yazigi (2014) Coordination interactions in the crystalline lattice of alkaline ions with the polyoxometalate $[V_{12}B_{18}O_{60}H_6]^{10-}$ ligand, Journal of Coordination Chemistry, 67:23-24, 3940-3952, DOI: 10.1080/00958972.2014.960407

To link to this article: http://dx.doi.org/10.1080/00958972.2014.960407

Journal of Coordination Chemistry, 2014
Vol. 67, Nos. 23–24, 3940–3952, http://dx.doi.org/10.1080/00958972.2014.960407

Coordination interactions in the crystalline lattice of alkaline ions with the polyoxometalate $[V_{12}B_{18}O_{60}H_6]^{10-}$ ligand

PATRICIO HERMOSILLA-IBÁÑEZ†‡, JUAN COSTAMAGNA†, ANDRÉS VEGA‡§, VERÓNICA PAREDES-GARCÍA‡§, ERIC LE FUR¶‖, EVGENIA SPODINE*‡†† and DIEGO VENEGAS-YAZIGI*†‡

†Facultad de Química y Biología, Universidad de Santiago de Chile, Santiago, Chile
‡CEDENNA, Santiago, Chile
§Facultad de Ciencias Exactas, Departamento de Ciencias Químicas, Universidad Andres Bello, Santiago, Chile
¶ENSCR, CNRS, UMR 6226, Rennes, France
‖Université Européenne de Bretagne, France
††Facultad de Ciencias Químicas y Farmacéuticas, Universidad de Chile, Santiago, Chile

(*Received 6 June 2014; accepted 24 July 2014*)

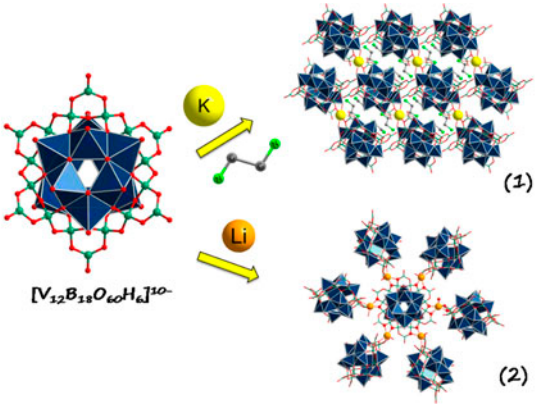

In the present work, the synthesis and structural characterization of two new polyoxovanadoborate (BVO) frameworks, based on the $[V_{12}B_{18}O_{60}H_6]^{10-}$ polyanion, are reported, $K(H_3O)(enH_2)_4[V_{12}B_{18}O_{60}H_6]\cdot 9.60H_2O$ (**1**) and $Li_8(NH_4)_2[V_{12}B_{18}O_{60}H_6]\cdot 8.02H_2O$ (**2**). Both compounds are obtained in a mixed valence ratio of $10V^{IV}/2V^{V}$. Framework **1** is characterized by potassium ions coordinated by the BVO cluster and ethylenediammonium and hydronium ions as charge-compensating agents. In framework **2**, the BVO clusters are coordinating lithium ions and the charge is compensated by ammonium ions. Using the SHAPE 2.1 program, it was possible to calculate the best geometry for the existing lithium and potassium ions. For **2**, the lithium ions are five-coordinate, best described by a square pyramid (SPY-5), while the coordination sphere around the potassium ions in **1** are six-coordinate. For **1**, the coordination sphere of the existing potassium ions in the framework can be described as trigonal prism (TPR-6). Calculations were also done for a previously reported cluster $[Na_{10}[(H_2O)V_{12}B_{18}O_{60}H_6]\cdot 18H_2O]$ (**3**), in which the sodium ions are

*Corresponding authors. Email: espodine@ciq.uchile.cl (E. Spodine); diego.venegas@usach.cl (D. Venegas-Yazigi)

six-coordinate but in two different geometries, these being octahedral and TPR-6. The influence of the interactions of the alkali ions with the $[V_{12}B_{18}O_{60}H_6]^{10-}$ polyanion, on the vanadate and borate absorption bands observed in the infrared spectra, is discussed.

Keywords: Polyoxometalate; Mixed valence; BVO; Lithium; $V_{12}B_{18}O_{60}$

1. Introduction

Polyoxometalates (POMs) are clusters that can act as ligands through many peripheral oxygens that they possess and can act as donors to different cationic species, such as alkali ions, alkaline earth ions, transition metal ions, and/or lanthanide ions. Thus, POMs, acting as multidentate polyanionic inorganic ligands, are used as building blocks to obtain structures that range from 0-D to supramolecular 3-D frameworks [1–10].

The mixed valence V^{IV}/V^{V} systems based on polyoxovanadoborate (VBO) POMs have attracted attention, and POMs with different vanadium to boron ratios can be found in the literature. Since the first BVO clusters were reported by Rijssenbeek in [11], several frameworks based on these clusters have appeared in the literature: V_6B_{20} [12–15], V_6B_{22} [16], $V_{10}B_{28}$ [17, 18], $V_{12}B_{16}$ [19–21], $V_{12}B_{17}$ [11], $V_{12}B_{18}$ [11, 16, 22–33], and $V_{12}B_{32}$ [34, 35], with the most frequently reported clusters V_6B_{20}, $V_{10}B_{28}$, $V_{12}B_{16}$ and $V_{12}B_{18}$.

Alkali ions and/or transition metal ions, or the corresponding complexes, are usually present in the crystalline lattice coordinated by the polyanions. They can be present only as charge-compensating species and sometimes together with protonated diamines. To the best of our knowledge, three crystalline lattices have been reported in the literature, in which only alkali ions are present coordinated by the VBO clusters, $Rb_4[(VO)_6\{B_{10}O_{16}(OH)_6\}_2]\cdot 0.5H_2O$ [12], $H_{15}[V_{12}B_{32}O_{84}Na_4]\cdot 13H_2O$ [34], and $[Na_{10}[(H_2O)V_{12}B_{18}O_{60}H_6]\cdot 18H_2O$ [30]. Continuing with our interest in understanding the role of these clusters acting as polydentate ligands toward transition metal ions and complexes, and alkali ions, we obtained two new frameworks with Li^+ and K^+. Herein, we report two new crystalline lattices, $K(H_3O)(enH_2)_4[V_{12}B_{18}O_{60}H_6]\cdot 9.60H_2O$ (**1**) and $Li_8(NH_4)_2[V_{12}B_{18}O_{60}H_6]\cdot 8.02H_2O$ (**2**), which are constructed by the bonding of $[V_{12}B_{18}O_{60}H_6]^{10-}$ to potassium, ethylenediammonium and hydronium ions (**1**), and lithium and ammonium ions in **2**. These networks will be compared with that based on sodium ions, $(Na)_{10}[V_{12}B_{18}O_{60}H_6]\cdot 19H_2O$ (**3**) [30–32], and the different coordination environments of the alkali ions will be also discussed.

2. Experimental

2.1. *Syntheses of compounds*

All chemicals were reagent grade and used without purification. Compound **1** was prepared in a 23 mL Teflon-lined Parr reactor by heating at 180 °C for 5 days, while **2** was also obtained in a 23 mL Teflon-lined Parr reactor, but heating at 170 °C for 3 days. After cooling to room temperature, dark red crystals of both compounds were collected by filtration. The crystals were washed with water and dried at room temperature.

2.1.1. $K(H_3O)(enH_2)_4[V_{12}B_{18}O_{60}H_6]\cdot 9.60H_2O$ (1). A mixture of V_2O_5 (0.1818 g, 1.00 mM), H_3BO_3 (1.0000 g, 16.0 mM), K_2HPO_4 (0.2612 g, 1.50 mM), $CrCl_3\cdot 6H_2O$ (0.5330 g, 2.00 mM), H_2O (2.0 mL, 111 mM), and ethylenediamine (0.4 mL, 6.00 mM)

was used to prepare **1**. The initial pH of the reacting mixture was 8.63, and the final value was 8.62. Yield: (0.2052 g, 55% based on V).

2.1.2. $Li_8(NH_4)_2[V_{12}B_{18}O_{60}H_6]\cdot 8.02H_2O$ (2). A mixture of NH_4VO_3 (0.2164 g, 1.85 mM), $Li_2B_4O_7$ (0.8354 g, 4.94 mM), H_2O (2.0 mL, 111 mM), and ethylenediamine (0.08 mL, 1.24 mM) was used to obtain **2**. Initial pH was 10.85, and the final value was 10.75. Yield: (0.0815 g, 26% based on V).

2.1.3. $Na_{10}[V_{12}B_{18}O_{60}H_6]\cdot 19H_2O$ (3). Compound **3** was obtained using the synthetic procedure reported by Brown *et al.* [30].

2.2. *Crystal structure determination*

For each compound, a single crystal was taken directly from the synthesis vessel. Examination under microscope suggested acceptable quality; these were mounted on the tip of a glass fiber. Preliminary examination with X-rays confirmed the quality suggested by microscopy, proceeding to full data collection. Data collection for **1** was performed at room temperature on a Bruker-Kappa-CCD diffractometer with graphite-monochromated Mo-Kα radiation ($\lambda = 0.71073$ Å). Intensities were collected by the program COLLECT [36]. Reflection indexing, Lorentz polarization correction, peak integration, and background determination were carried out with the DENZO program of the Kappa-CCD software package [37]. Unit-cell parameters, refinement, and frame scaling were performed with the program DIRAX/LSQ [38]. Data integration and scaling of the reflections were performed with the suite SCALEPACK [39]. The intensities for **2** were recorded at room temperature on a Bruker Smart Apex diffractometer using separations of 0.3° between frames and 10s by frame. Data integration were made using SAINTPLUS [40]. The structures were solved by direct methods using XS in SHELXTL [41] and completed (non-H atoms) by Fourier difference synthesis. Refinement until convergence were obtained using XL SHELXTL [42] and SHELXL97 [43]. The H-atom positions were calculated after each cycle of refinement using a riding model, with C–H = 0.97 Å and $U_{iso}(H) = 1.2\ U_{eq}$(parent) and N–H = 0.89 or 0.91 Å and $U_{iso}(H) = 1.5\ U_{eq}$(parent). Efforts to locate the borovanadate hydrogens in the final Fourier difference map were unsuccessful; those reported for the formula are based on charge-balance analysis. For **1**, the 10.60 oxygens occupy 18 positions. No hydrogens from the hydronium ions or water were located in the final difference Fourier map. For **2**, the occupancy of lithiums Li1, Li2, and Li3 was refined and finally set to 0.60, 0.90, and 0.80, respectively. No hydrogens from the ammonium ions or water were located in the final difference Fourier map. Efforts to lower the rather high residuals on the refinement for each compound included the evaluation of different models of solvation, and the use of squeeze for the modeling of the remaining density was unsuccessful. Some parameters remained high; this should be considered as arising from the complexity of the model used for the solvation and counterbalancing. Moreover, it is not related to the main characteristics of the structures, whose determination should still be considered as correct. The crystal data and structure refinement for **1** and **2** are summarized in table 1. For the crystallographic description, distances up to 3.1 Å were considered to define hydrogen bonds in the crystalline lattice [44]. For the crystallographic discussion of **3,** the crystallographic information file provided by the Cambridge Crystallographic Data Center was used

Table 1. Crystal data and structure refinement for **1** and **2**.

Complex	**1**	**2**
Formula	$C_8H_{68.2}B_{18}K\ N_8O_{70.60}V_{12}$	$B_{18}H_{30.04}Li_8N_2O_{68.02}V_{12}$
Moiety formula	$K(H_3O)(enH_2)_4[V_{12}B_{18}O_{60}H_6]\cdot 9.60H_2O$	$Li_8(NH_4)_2[V_{12}B_{18}O_{60}H_6]\cdot 8.02H_2O$
Formula weight	2251.60	2007.99
Temperature (K)	293(2)	297(2)
Crystal system	Monoclinic	Cubic
Space group	$C2/_C$	*Pn-3*
a (Å)	22.784(1)	18.8424(7)
b (Å)	14.847(1)	18.8424(7)
c (Å)	21.946(1)	18.8424(7)
α (°)	90.00	90.00
β (°)	108.72(1)	90.00
γ (°)	90.00	90.00
Volume (Å^3)	7030.6(3)	6689.7(4)
Z	4	2
Density (Calcd) (g cm^{-3})	2.100	1.970
Absorption coefficient (mm^{-1})	1.715	1.722
F (0 0 0)	4375.2	3816.7
Crystal size (mm^3)	0.27 × 0.20 × 0.10	0.32 × 0.17 × 0.16
θ range for data collection (°)	3.54–27.5	1.87–25.97
Index ranges	$-29 \le h \le 29$, $-19 \le k \le 18$, $-28 \le l \le 28$	$-23 \le h \le 23$, $-23 \le k \le 23$, $-23 \le l \le 23$
Reflections collected	34,591	43,467
Independent reflections	8082 [*R*(int) = 0.0579]	2204 [*R*(int) = 0.0404]
Refinement method	Full-matrix least-squares on F^2	Full-matrix least-squares on F^2
Goodness-of-fit on F^2	1.043	1.178
Final *R* indices [$I > 2\sigma(I)$]	$R_1 = 0.0660$, $wR_2 = 0.1792$	$R_1 = 0.0702$, $wR_2 = 0.2182$
R indices (all data)	$R_1 = 0.1030$, $wR_2 = 0.2095$	$R_1 = 0.0738$, $wR_2 = 0.2228$
Largest diff. peak/hole (e Å^{-3})	2.49/−1.13	2.46/−0.48

(CCDC-727716). Structure drawings were carried out with DIAMOND-3.2i, supplied by Crystal Impact [45].

In order to describe the geometries around the alkaline ions found in the different frameworks, the methodology of the continuous shape measures algorithm [46], the minimal distortion paths [47], and the generalized interconversion coordinates [48] were used, as established in the SHAPE code [49].

2.3. *Physical measurements*

IR spectra of the compounds were determined on a Perkin Elmer FTIR spectrophotometer, model BX II, from 4000 to 400 cm^{-1} using KBr pellets. The UV–vis spectra for **1** and **2** were obtained at room temperature from 200 to 850 nm using a Lambda 1050 Wideband UV–vis–NIR spectrophotometer equipped with a diffuse reflectance attachment (Biconical DRA-CA-50M). The absorbance values were obtained by the use of the Kubelka–Munk function [50].

3. Results and discussion

3.1. *Syntheses*

The preparation of framework **1** was done at 180 °C for 5 days. At lower temperatures (170 °C) and fewer days of reaction (3 days), framework **2** was obtained.

The synthetic method to obtain **1** was done in the presence of a transition metal salt. The purpose to this salt was to obtain a framework with Cr^{III} and potassium ions coordinated by the polyanionic cluster. Although the transition metal ions did not bind to the polyanionic clusters or remain within the crystal lattice, their presence was absolutely necessary for the formation of the respective crystalline packing [20]. Both syntheses were done using V^{V} source; however, mixed valence clusters were obtained due to the presence of the added diamine that acts as a reducing agent. Only **1** has protonated amines in the crystalline framework, while **2** resulted in a pure inorganic one.

3.2. *Description of crystal structures*

Lattices **1**, **2**, and **3** present the polyanionic multidentate $[V_{12}B_{18}O_{60}H_6]^{10-}$ coordinated to alkali ions. **1** also has protonated ethylenediamine cations, which interact with the clusters through hydrogen bonds. The BVO can be described as formed by two hexanuclear oxovanadates $[V_6O_9]^{n+}$, condensed to a central $[B_{18}O_{36}(OH)_6]^{24-}$ ring. All vanadiums are five-coordinate, and each VO_5 unit has [4 + 1] geometry [51] and is condensed to another VO_5 unit through edges. The central borate ring is formed by six B_3O_7 moieties, each with one trigonal boron ($B_{trig,}$ Δ) and two tetrahedral ones ($B_{tet,}$ T). The nomenclature for the topology of the central borate fragment is 18[6Δ + 12T] [52, 53].

3.1.1. Structural description of $K(H_3O)(enH_2)_4[V_{12}B_{18}O_{60}H_6]\cdot 9.60H_2O$ (1). Two different crystallographic types of ethylenediammonium cations are present in the crystal packing of **1**. Both cations connect three clusters and two water molecules through hydrogen bonds. The first with four bifurcated and two single bonds (figure S1, see online supplemental material at http://dx.doi.org/10.1080/00958972.2014.960407) and the second with one bifurcated and five single bonds (figure S2). The hydrogen bond interactions scheme and distances between the cations, cluster units, and water molecules in the lattice can be seen in figures S3 and S4, and table S1. Each type of crystallographically different protonated diamine is oriented in the same direction in the lattice (figure 1).

This crystal lattice contains a potassium cation coordinated by the polyanionic ligand. K1 is six-coordinate symmetrically by two clusters (POM1 and POM2) through the following bonds: K1–O7 (vanadyl oxygen), K1–O9 (vanadyl oxygen), and K1–O25 (a bridging oxygen between a trigonal and a tetrahedral boron), with distances of 2.775, 2.866, and 2.852 Å, respectively (figure 2).

3.1.2. Structural description of $Li_8(NH_4)_2[V_{12}B_{18}O_{60}H_6]\cdot 8.02H_2O$ (2). In **2**, the connectivity of the polyanionic clusters coordinating the lithium cations is gained by the presence of ammonium ions and water molecules. This lattice is characterized by three different crystallographic types of Li ions. Li1 is five-coordinate with four oxygens donated by two BVO ligands (B_{trig}-O9-B_{tet} and B_{tet}-O7-B_{tet}), while the fifth oxygen corresponds to a water. Each polyanionic cluster is surrounded by six Li1 ions, which are crystallographically equivalent (figure 3). Li2 is also five-coordinate, but it is bonded to three BVO clusters, by two oxygens from vanadyl groups: O3=V (BVO1), O6=V (BVO2), one bridging oxygen B_{trig}-O9-B_{tet} (BVO2) and one terminal oxygen O10-B_{trig} (BVO3); the coordination sphere is completed by a water molecule (figure 4).

Li3 is six-coordinate, formed with equidistant Li3–O10 bonds (3.142 Å; B_{trig}-O10), where each oxygen belongs to a different BVO cluster [figure 5(a)]. These oxygens adopt a

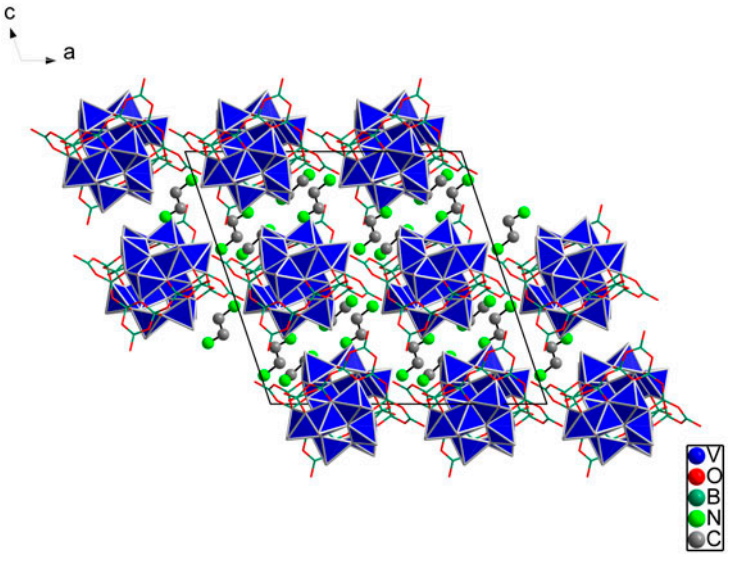

Figure 1. View of the crystalline packing of **1** in the plane (0 $\bar{1}$ 0).

chair conformation, as shown in figure 5(b). This six-coordinate mode has long distances (3.142 Å); lithium in crown ethers (15-crown-5) can also be six-coordinate, five oxygens from the crown ether and one chloride; all the lithium–oxygen distances are shorter (2.08–2.28 Å) [54]. Taking this into account, it is better to classify the observed distances for this ion as a pseudo-coordinative interaction.

The perpendicular view to the *bc* plane shows the position of the ammonium and lithium ions in the framework [figure S5(a)], while figure S5(b) shows that of the BVO clusters.

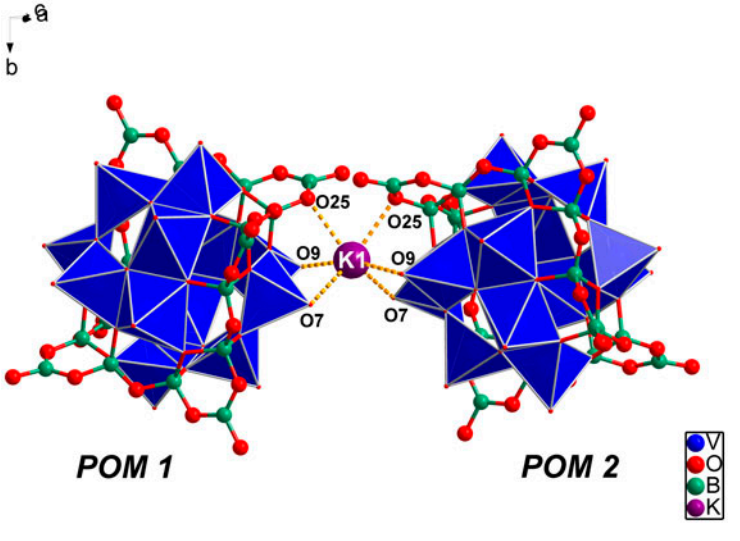

Figure 2. Coordination sphere of K1 for **1**.

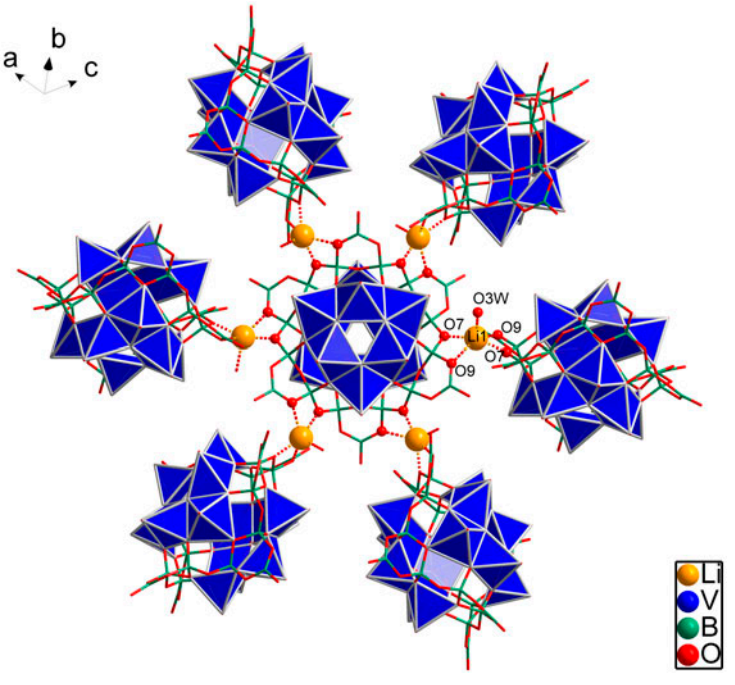

Figure 3. Coordination sphere of Li1 for **2**.

Two types of cavities formed by the BVO clusters alternate in the *bc* plane. Cavity 1 is formed by the oxygens provided by B_{tet}-O7-B_{tet} moieties and are filled by coordinated Li1 ions and water molecules. Cavity 2 is formed by the O3 atoms which belong to vanadyl groups, being occupied by ammonium ions and water molecules.

By taking into account the cations present in the lattices of **2** and **3**, they can be considered as completely inorganic. Framework **2** has also NH_4^+ ions which are responsible for the charge compensation. On the other hand, **1** can be considered as a hybrid lattice in which enH_2^{2+} and H_3O^+ are the countercations.

3.3. *Comparative description of the geometries around the alkaline ions*

The alkali ions in **1–3** have different coordination numbers. Using the SHAPE 2.1 program, developed by Alvarez *et al.* [49], it was possible to establish the best geometry for the existing lithium, potassium, and sodium ions. For **2**, the lithium ion is five-coordinate in a square pyramidal geometry (SPY-5), while the coordination spheres around the potassium (**1**) and sodium (**3**) ions are six-coordinate. The coordination sphere of the potassium ions can be described as trigonal prism (TPR-6), and that of the sodium ions as octahedral (OC-6) and TPR-6. All these coordination numbers for the alkali ions have been previously reported by Delgado *et al.* [55]. The obtained geometries of the alkali ions are shown in figure 6.

Based on the bond valence sum method [56], and using the crystallographic data, the mixed valence states of all the characterized clusters can be identified with the ratio of 10/2 (V^{IV}/V^{V}), since the calculated mean values were 4.16 for **1** and 4.14 for **2**, which are close

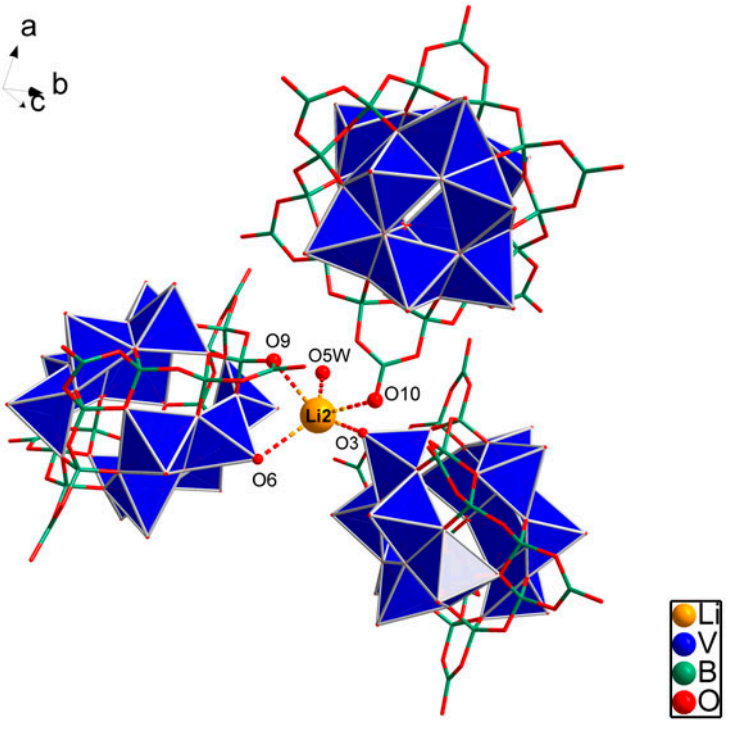

Figure 4. Coordination sphere of Li2 for **2**.

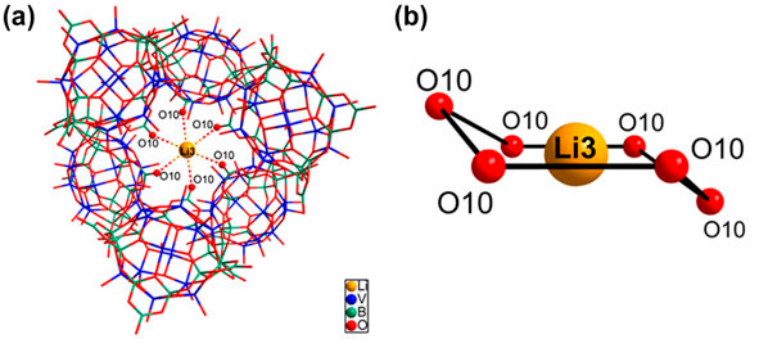

Figure 5. The oxygens adopt a chair conformation for Li3 in **2**.

to the expected value of 4.17 for 10 vanadium(IV) and two vanadium(V) centers. For **3**, a value of 4.24, which is also close to the expected value, was previously reported [30].

3.4. *FTIR spectrum*

Compounds **1**, **2**, and **3** show the same features in the FTIR spectra from 1500 to 600 cm^{-1}, where the main absorption bands correspond to $\nu_{B-O\ (BO3)}$, $\nu_{B-O\ (BO4)}$, $\nu_{V=O}$, ν_{V-O-V} of the

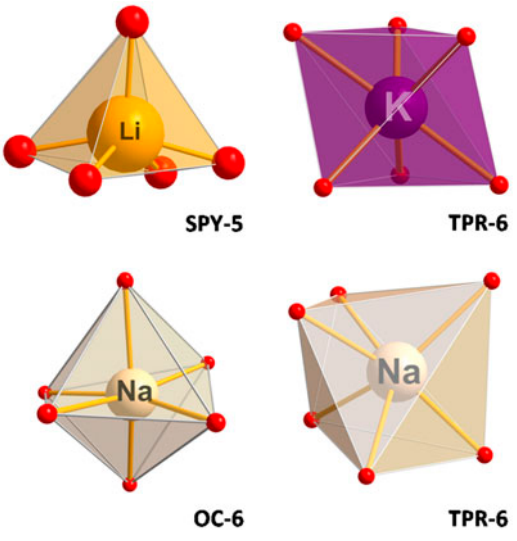

Figure 6. The different geometries of the alkali ions; SPY-5 (square pyramid), OC-6 (octahedron), and TPR-6 (trigonal prism).

$[V_{12}B_{18}O_{60}H_6]^{10-}$ polyanionic cluster (figure S6, table 2). The bands associated to the ν_{V-O-V} vibration in the above-mentioned cluster are shifted to lower wavelengths, as compared to a pure oxovanadium system, where they appear at 818 and 742 cm^{-1} [57]. The pattern of bands in the characteristic region of the terminal oxovadium group shows an asymmetric band at 941–952 and 885–892 cm^{-1} for the three studied lattices and is attributed to the presence of V^V and V^{IV}, respectively. In the three studied spectra, the bands are broad enough that the lower energy band appears as a shoulder, instead of a well-defined band, as reported by Keene *et al.* [57]. This can be interpreted as corresponding to more delocalized systems than the one reported by Keene [57].

The nature of the countercations in the lattice for **1** (K^+, enH_2^{2+}), **2** (Li^+), and **3** (Na^+) produces different shifts in the values of the corresponding absorption bands of the vanadyl groups.

As stated before, in **2,** the distances between Li1 to B_{tet}-O-B_{tet} and Li1 to B_{trig}-O-B_{tet} are 1.921 and 2.303 Å, respectively. Li2 is also within bonding distance with B_{trig}-O-B_{tet} and terminal B_{trig}-O (2.894 and 2.902 Å). The vibrations associated to bridging oxygens are affected by the stronger coordination of Li1 (shortest distance), and this is evidenced with the increase of the vibration energy of the B–O–B bands (1097–1053 cm^{-1}).

Table 2. Most relevant absorption bands in the FTIR spectra and the corresponding assignments for **1**, **2**, and **3**.

Compound	Cation	$\nu_{B-O\ (BO3)}$ (cm^{-1})	$\nu_{B-O\ (BO4)}$ (cm^{-1})	$\nu_{V=O}$ (cm^{-1})	ν_{V-O-V} (cm^{-1})
1	K^+, enH_2^{2+}	1398,1353	1082,1041	941,885	779,635
2	Li^+	1403,1373	1097,1053	952,891	792,610
3	Na^+	1414,1358	1087,1048	951,892	789,611

Table 3. Bond distances from the oxygen atoms of the ligands to the alkaline cations in **1**, **2**, and **3**.

Compound	Alkaline ion	Bond to BVO cluster	Distance (Å)	Type of bond
1	K^+	K1–O7	2.775	vanadyl oxygen
		K1–O9	2.866	vanadyl oxygen
		K1–O25	2.852	B_{trig}-O25-B_{tet}
2	Li^+	Li1–O7	1.921	B_{tet}-O7-B_{tet}
		Li1–O9	2.303	B_{trig}-O9-B_{tet}
		Li2–O3	2.816	vanadyl oxygen
		Li2–O6	2.976	vanadyl oxygen
		Li2–O9	2.894	B_{trig}-O9-B_{tet}
		Li2–O10	2.902	B_{trig}-O10
		Li3–O10	3.142	B_{trig}-O10
3	Na^+	Na1–O6	2.415	B_{trig}-O6-B_{tet}
		Na1–O24	2.771	O-μ3 (2V, 1B_{tet})
		Na1–O9	2.487	vanadyl oxygen
		Na1–O11	2.451	vanadyl oxygen
		Na1–O16	2.753	O-μ3 (2V, 1B_{tet})
		Na1–O30	2.395	B_{trig}-O30-B_{tet}
		Na2–O7	2.392	vanadyl oxygen
		Na2–O11	2.362	vanadyl oxygen
		Na2–O15	2.481	B_{trig}-O15
		Na3–O14	2.748	B_{trig}-O14
		Na3–O29	2.316	B_{trig}-O29-B_{tet}
		Na3–O18	2.404	vanadyl oxygen
		Na4–O19	2.484	B_{trig}-O19
		Na4–O12	2.902	B_{trig}-O12-B_{tet}
		Na4–O7	2.734	vanadyl oxygen
		Na4–O10	2.461	vanadyl oxygen
		Na5–O9	2.562	vanadyl oxygen
		Na5–O3	2.458	B_{tet}-O3-B_{tet}
		Na5–O30	2.528	B_{trig}-O30-B_{tet}

Thus, these two lithium ions are within a coordinative distance to the oxygens of the borate groups and therefore affect the vibrations of these groups as shown in table 3. When one compares the borate absorption bands of **2** with those of **1**, a shift is observed that should account for the proximity of the lithium ions to the clusters. Thus, **1** and **3** (this last one completely an inorganic framework with sodium ions in the crystalline lattice) can be considered as examples in which the alkali ions are bonded to the peripheral oxygens of the cluster, and therefore affecting the stretching vibrations of the borate groups.

3.5. *Reflectance UV–visible spectra*

Due to the insolubility of the compounds, the solid diffuse reflectance UV–visible spectra were recorded (figure 7). All the studied compounds crystallize as dark red crystals and gave similar UV–visible spectra, as previously reported by Hermosilla-Ibañez *et al.* [58]. The absorption centered at 555 nm for the three studied compounds was assigned to an intervalence charge transfer transition (IVCT) between the V^{IV}/V^{V} centers of the BVO unit. The absorptions observed in the high-energy UV region were assigned to O → V charge transfer at 5.19 eV (239 nm) for **1** and 5.08 eV (244 nm) for **2**, and to O → B charge transfer at 3.89 eV (319 nm) for **1** and 3.99 eV (311 nm) for **2** [32]. Therefore, the electronic absorptions observed in the solid state seem to be dependent only of the BVO moiety and the characteristics of the lattice have little influence on the optical properties.

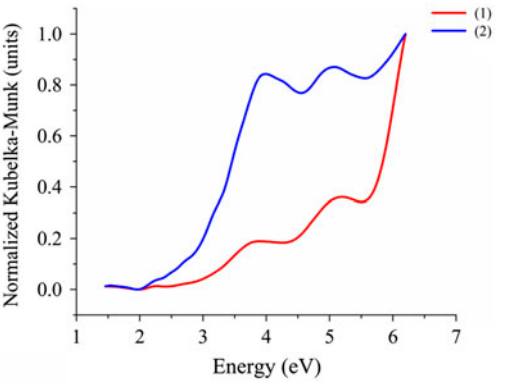

Figure 7. UV–vis reflectance spectra for **1** and **2**.

4. Conclusion

All compounds can be described as having a mixed valence ratio of $10V^{IV}/2V^{V}$ and different geometrical environments for the alkali ions in the frameworks.

The nature of the countercations in the lattice for **1** (K^+), **2** (Li^+), and **3** (Na^+) produces different shifts in the values of the corresponding absorption bands of the vanadyl groups in the infrared spectra. The sodium framework possesses a higher number of coordination interactions, and therefore the greater shift of the vanadyl stretch.

When one compares the borate absorption bands of **2** with those of **1** in the infrared spectra, a shift is observed that should be accounted by coordination of the lithium ions to the clusters.

The observed electronic absorptions in the solid state correspond to the BVO moiety, while the characteristics of the lattice have little influence on the optical properties.

The BVO clusters are good ligands, as can be observed in **2,** where six polyoxo ligands present a pseudo-coordinative interaction with one lithium ion with distances of c.a. 3.0 Å.

Supplementary material

Additional figures, tables, and crystallographic data for structures of **1** and **2** reported in this paper have been deposited with the Cambridge Crystallographic Data Center as supplementary publication number CCDC-932258, 963462. Copies of the data can be obtained free of charge on application to CCDC, 12 Union Road Cambridge CB21EZ, UK (Fax: int. code +44 (123) 336 033; E-mail: deposit@ccdc.cam.ac.uk.

Acknowledgments

Authors acknowledge FONDECYT 1120004 for financial support. This work was done under the LIA-MIF CNRS 836 Collaborative Program. PHI thanks MECESUP UCH 0601 Doctoral Scholarship. PHI also thanks CONICYT AT-24100222 and TT-23120099 Doctoral Scholarships. Authors are indebted to T. Roisnel for X-ray data collection of **1**.

References

[1] D.L. Long, R. Tsunashima, L. Cronin. *Angew. Chem. Int. Ed.*, **49**, 1736 (2010).
[2] F. Li, L. Xu. *Dalton Trans.*, **40**, 4024 (2011).
[3] C. Pichon, A. Dolbecq, P. Mialane, J. Marrot, E. Rivière, F. Sécheresse. *Dalton Trans.*, 71 (2008).
[4] S. Romo, N.S. Antonova, J.J. Carbó, J.M. Poblet. *Dalton Trans.*, **2008**, 5166 (2008).
[5] S. Inami, M. Nishio, Y. Hayashi, K. Isobe, H. Kameda, T. Shimoda. *Eur. J. Inorg. Chem.*, 5253 (2009).
[6] W. Chen, Y. Li, Y. Wang, E. Wang, Z. Zhang. *Z. Anorg. Allg. Chem.*, **635**, 1678 (2009).
[7] H.M. Zhang, Y.G. Li, Y. Lu, R. Clérac, Z.M. Zhang, Q. Wu, X.J. Feng, E.B. Wang. *Inorg. Chem.*, **48**, 10889 (2009).
[8] S.G. Mitchell, P.I. Molina, S. Khanra, H.N. Miras, A. Prescimone, G.J. Cooper, R.S. Winter, E.K. Brechin, D.L. Long, R.J. Cogdell, L. Cronin. *Angew. Chem. Int. Ed.*, **50**, 9154 (2011).
[9] G. Zhu, Y.V. Geletii, C. Zhao, D.G. Musaev, J. Song, C.L. Hill. *Dalton Trans.*, **41**, 9908 (2012).
[10] M. Nishio, S. Inami, Y. Hayashi. *Eur. J. Inorg. Chem.*, **2013**, 1876 (2013).
[11] J.T. Rijssenbeek, D.J. Rose, R.C. Haushalter, J. Zubieta. *Angew. Chem. Int. Ed. Engl.*, **36**, 1008 (1997).
[12] C.J. Warren, J.T. Rijssenbeek, D.J. Rose, R.C. Haushalter, J. Zubieta. *Polyhedron*, **17**, 2599 (1998).
[13] I.D. Williams, M. Wu, H.H. Sung, X.X. Zhang, J. Yu. *Chem. Commun.*, **1998**, 2463 (1998).
[14] Y.N. Cao, H.H. Zhang, C.C. Huang, Y.X. Sun, Y.P. Chen, W.J. Guo, F.L. Zhang. *Chin. J. Struct. Chem.*, **24**, 525 (2005).
[15] Q. Cai, B. Lu, J. Zhang, Y. Shan. *J. Chem. Crystallogr.*, **38**, 321 (2008).
[16] X. Liu, J. Zhou, L. An, R. Chen, F. Hu, Q. Tang. *J. Solid State Chem.*, **201**, 79 (2013).
[17] M. Wu, T.S. Law, H.H. Sung, J. Cai, I.D. Williams. *Chem. Commun.*, **2005**, 1827 (2005).
[18] Y. Cao, H. Zhang, C. Huang, Q. Yang, Y. Chen, R. Sun, F. Zhang, W. Guo. *J. Solid State Chem.*, **178**, 3563 (2005).
[19] C.J. Warren, R.C. Haushalter, D.J. Rose, J. Zubieta. *Inorg. Chim. Acta*, **282**, 123 (1998).
[20] Y. Cao, H. Zhang, C. Huang, Y. Chen, R. Sun, W. Guo. *J. Mol. Struct.*, **733**, 211 (2005).
[21] G. Li, H. Mei, S. Deng, Y. Sun, H. Hu, Y. Chen, H. Zhang. *Spectrosc. Spect. Anal.*, **31**, 3026 (2011).
[22] L. Zhang, Z. Shi, G. Yang, X. Chen, S. Feng. *J. Solid State Chem.*, **148**, 450 (1999).
[23] Z. Lin, H. Zhang, C. Huang, R. Sun, Y. Chen. *Acta Chim. Sinica*, **62**, 391 (2004).
[24] Z. Lin, H. Zhang, C. Huang, R. Sun, Q. Yang. *Chin. J. Struct. Chem.*, **23**, 83 (2004).
[25] Z. Lin, Q. Yang, H. Zhang, C. Huang, R. Sun, X Wu. *Chin. J. Struct. Chem.*, **23**, 590 (2004).
[26] B. Lu, H. Wang, L. Zhang, C. Dai, Q. Cai, Y. Shan. *Chin. J. Chem.*, **23**, 137 (2005).
[27] X. Liu, J. Zhou. *Z. Naturforsch.*, **66**, 0115 (2011).
[28] X. Liu, J. Zhou, Z. Zhou, F. Zhang. *J. Cluster Sci.*, **22**, 65 (2011).
[29] G. Li, H. Mei, X. Chen, Y. Chen, Y. Sun, H. Zhang, X. Chen. *Chin. J. Struct. Chem.*, **30**, 785 (2011).
[30] K. Brown, P.E. Car, A. Vega, D. Venegas-Yazigi, V. Paredes-García, M.G.F. Vaz, R.A. Allao, J. Pivan, E. Le Fur, E. Spodine. *Inorg. Chim. Acta*, **367**, 21 (2011).
[31] J. Zhou, X. Liu, F. Hu, H. Zou, X. Li. *Inorg. Chem. Commun.*, **25**, 51 (2012).
[32] J. Zhou, X. Liu, F. Hu, H. Zou, R. Li, X. Li. *RSC Advances*, **2**, 10937 (2012).
[33] J. Zhou, X. Liu, R. Chen, H. Xiao, F. Hu, H. Zou, Y. Zhou, C. Liu, L. Zhu. *CrystEngComm*, **15**, 5057 (2013).
[34] T. Yamase, M. Suzuki, K. Ohtaka. *J. Chem. Soc., Dalton Trans.*, 2463 (1997).
[35] C.J. Warren, D.J. Rose, R.C. Haushalter, J. Zubieta. *Inorg. Chem.*, **37**, 1140 (1998).
[36] Nonius. *COLLECT*, Nonius BV, Delft, The Netherlands (1998).
[37] Nonius. *Kappa CCD Program Package: SCALEPACK, SORTAV*, Nonius BV, Delft, The Netherlands (1999).
[38] A.J.M. Duisenberg, L.M.J. Kroon-Batenburg, A.M.M. Schreurs. *J. Appl. Crystallogr.*, **36**, 220 (2003). (EVAL-CCD).
[39] A.J.M. Duisenberg. *J. Appl. Crystallogr.*, **25**, 92 (1992).
[40] *SAINTPLUS (Version 6.02)*, Bruker AXS, Madison, WI (1999).
[41] *SHELXTL (Version 5.1)*, Bruker AXS, Madison, WI (1998).
[42] G.M. Sheldrick. *Acta Crystallogr., Sect. A: Found. Crystallogr.*, **64**, 112 (2008).
[43] G.M. Sheldrick. *SHELXL-97, Program for Crystal Structure Refinement*, University of Göttingen, Germany (1997).
[44] G.R. Desiraju, T. Steiner. *The Weak Hydrogen Bond: In Structural Chemistry and Biology*, Oxford University press, Oxford (2001).
[45] K. Brandenburg. *DIAMOND, Version 3.2i*, Crystal Impact GbR, Bonn (2012).
[46] M. Pinsky, D. Avnir. *Inorg. Chem.*, **37**, 5575 (1998).
[47] D. Casanova, J. Cirera, M. Llunell, P. Alemany, D. Avnir, S. Alvarez. *J. Am. Chem. Soc.*, **126**, 1755 (2004).
[48] J. Cirera, E. Ruiz, S. Alvarez. *Chem. Eur. J.*, **12**, 3162 (2006).
[49] M. Llunell, D. Casanova, J. Cirera, P. Alemany, S. Alvarez. *SHAPE (version 2.1)*, Universitat de Barcelona, Barcelona (2013).
[50] W.W. Wendlandt, H.G. Hecht. *Reflectance Spectroscopy*, Wiley-Interscience, New York (1966).
[51] P.J. Hagrman, R.C. Finn, J. Zubieta. *Solid State Sci.*, **3**, 745 (2001).
[52] C.L. Christ, J.R. Clark. *Phys. Chem. Miner.*, **2**, 59 (1977).

[53] G. Yuan, D. Xue. *Acta Crystallogr., Sect. B: Struct. Sci.*, **63**, 353 (2007).
[54] P.C. Stark, M. Huff, E.A. Babaian, L.M. Barden, D.C. Hrncir, S.G. Bott, J.L. Atwood. *J. Inclusion Phenom.*, **5**, 683 (1987).
[55] F.S. Delgado, C. Ruiz-Pérez, J. Sanchiz, F. Lloret, M. Julve. *CrystEngComm*, **8**, 507 (2006).
[56] I.D. Brown, D. Altermatt. *Acta Crystallogr., Sect. B: Struct. Sci.*, **41**, 244 (1985).
[57] T.D. Keene, D.M. D'Alessandro, K.W. Krämer, J.R. Price, D.J. Price, S. Decurtins, C.J. Kepert. *Inorg. Chem.*, **51**, 9192 (2012).
[58] P. Hermosilla-Ibáñez, P.E. Car, A. Vega, J. Costamagna, F. Caruso, J.Y. Pivan, E. Le Fur, E. Spodine, D. Venegas-Yazigi. *CrystEngComm*, **14**, 5604 (2012).